

A Unified Distance Measure Scheme for Orientation Coding in Identification

Shaoqiu Zheng and Ying Tan, *Senior Member, IEEE*

Abstract—For a recognition task, distance measure between patterns is one of the most important procedures. Orientation coding-based methods have achieved high accuracy and speed in recognition, such as competitive code, palmprint orientation code and robust line orientation code. For orientation coding-based patterns, OR_XOR (Hamming distance) and SUM_XOR (Angular distance) are usually used for measuring the distance. However, little work have been done to study the physical significance of these distances for orientation coding-based patterns. The relationship between SUM_XOR and OR_XOR is not clear. This paper is focusing on the relationship between them and proposes a unified distance measure (UDM) scheme. To automatically compute the parameters introduced in UDM model, the population based heuristic algorithms, particle swarm optimization (PSO), differential evolution (DE) and fireworks algorithm (FWA) are used for the determination of parameters. Experimental results on artificial date set, PolyU palmprint database and the collected finger-vein database, suggest that the proposed PSO-UDM, DE-UDM, FWA-UDM gain lower equal error rate.

I. INTRODUCTION

PERSONAL identification is a key issue in human's daily life. Recently, the authentication by biometric characteristics is becoming more and more popular due to their high accuracy and easy implementation. Face [1], iris [2], palmprint [3], [4], finger print [5], speech [6] and finger-veins [7], [8] are the favorite intrinsic physical traits in human body and have been widely investigated. For biometrics, how to effectively represent the features is one of the principal issues for an authentication problem. Among the traits, recent works on representing the palmprint and finger-vein features both focus on extracting the line shape patterns. For finger-vein trait, the line shape pattern is the vein structure, and the line shape pattern is the palm lines for palmprint.

Finger-vein recognition is a new developed technology for identification proposed by Miura et al. [7], [8]. Statistical investigation indicates that finger-vein structure is one of the unique patterns. People have different finger-vein structures and they will suffer little changes with age [9]. Moreover, finger-veins are inside the skin which render it more safer compared with other biometrics. To effetely extract the vein

This work was supported by the National Natural Science Foundation of China under grants number 61170057 and 60875080. The authors acknowledge The Polytechnic University of Hong Kong for providing the PolyU Palmprint database.

The authors are with the Key Laboratory of Machine Perception (Ministry of Education) and Department of Machine Intelligence, School of Electronics Engineering and Computer Science, Peking University, Beijing 100871, China. Email: {zhengshaoqiu, ytan}@pku.edu.cn. Y. Tan is the corresponding author.

patterns, many algorithms have been proposed, repeat line tracking [7], [10], [11], pattern extraction by convoluting the images with designed filters [12], [13], maximum curvature point methods [8], [14], and machine learning algorithms [15], [16].

For palmprint recognition, recently, orientation coding-based methods have been proposed and have gained great success compared with other algorithms for representing the line-shape feature [17]–[19]. These algorithms used a bank of filters with different orientations to convolute with the palmprint images. The orientation is recoded as orientation values by the dominate convolution results to represent patterns.

For a recognition target, it usually includes the preprocessing of the captured images, pattern extraction, distance computation and decision making. A successful implementation of a recognition system is influenced by all the steps. Thus, the distance measure between two patterns is also a principal step. An effective distance measure scheme can greatly increase the accuracy and the speed. To compute the distances among these orientation coding-based patterns, SUM_XOR (angle distance) and OR_XOR (hamming distance) are usually used. In [17], Kong et al. proposed competitive code (CompCode) algorithm for pattern extraction and SUM_XOR was used as distance measure scheme for patterns. In [19], Wu et al. designed a set of artificial templates with different orientation for line detection, and encoded the pattern by the minimal response direction, which was palmprint orientation code (POC). They used OR_XOR for the computation of distance. In [18], Jia et al. used the modified finite radon transform for pattern extraction, which was named robust line orientation code (RLOC). OR_XOR was used to compute the distance.

Even though the orientation based algorithms have gained success in biometrics identification, there is little work on the distance measure schemes. In [20], Kong pointed out that SUM_XOR usually performs better than OR_XOR in palmprint database, but is it always so in all the databases? In [21], Guo et al. tried to use a unified distance measure for recognition, however, the physical meaning of the unified distances measure scheme is not explained. Moreover, the relation between OR_XOR and SUM_XOR is not clear. The rest of this paper will stress concentration on these questions.

As pointed out previously, pattern extraction for finger-vein is to effectively represent the line-shape structure. The orientation coding-based methods have gained great success in palmprint identification. Thus, in the following experiments, the collected finger-vein data set is also used to validate the

proposed distance measure scheme.

Following this introductory section, we present the relation between hamming distance and angular distance, and a unified distance model is proposed. To determine the parameters introduced in the model, population based heuristic algorithms are used for the optimization of the parameters in Section II. Section III illustrates the performance comparison on three databases, artificial binary data set, PolyU palmprint database and the collected finger-vein images database. In Section IV, we study the influences of the parameters and give explanations of the setting of the parameters in UDM model. Finally, conclusion is drawn in section V.

II. THE PROPOSED DISTANCE MEASURE SCHEME

Distance measure is one of the principal procedures for a recognition target, and should be in unison with the pattern extraction algorithm. Previous work used *SUM_XOR* and *OR_XOR* to calculate the distance. However, the details of the distance measure schemes are not studied. In the following, we will stress the physical significances of them.

A. Relation Between *SUM_XOR* And *OR_XOR*

Denote $I(x, y)$ is the pre-processed image, the pattern image $P(x, y)$ is computed as

$$P(x, y) = \arg \min_{\forall i \in [0, N-1]} I(x, y) \otimes G(x, y, \theta_i) \quad (1)$$

where \otimes is the convolution operation. Suppose $N = 6$, then $\theta_i = i\pi/6$. Each point in $P(x, y)$ is the orientation θ_i with the dominant response, and the distance between two pattern images $P(x, y), Q(x, y)$ is sum of the distance of all corresponding points. Here, some basic rules are presented firstly. θ_a and θ_b are two corresponding points in $P(x, y)$ and $Q(x, y)$.

- 1) $d(\theta_a, \theta_b) = d(\theta_b, \theta_a)$ (Symmetry).
- 2) $d_0 = d(\theta_a, \theta_a) = 0$.
- 3) $d_1 = d(0, \pi/6) = d(\pi/6, \pi/3) = d(\pi/3, \pi/2) = d(\pi/2, 2\pi/3) = d(2\pi/3, 5\pi/6) = d(5\pi/6, 0)$. For any two orientation, the interval between $\pi/6$ should be equal.
- 4) $d_2 = d(0, \pi/3) = d(\pi/6, \pi/2) = d(\pi/3, 2\pi/3) = d(\pi/2, 5\pi/6) = d(2\pi/3, 0)$
For any two orientation, the interval between $\pi/3$ should be equal.
- 5) $d_3 = d(0, \pi/2) = d(\pi/6, 2\pi/3) = d(\pi/3, 5\pi/6) = d(\pi/2, 5\pi/6)$
For any two orientation, the interval with $\pi/2$ should be equal.

To represent the orientation, Kong et al. used a 3 bits ($\log_2 6$) encode method for orientation coding [17], which encode the orientations $\{0, \pi/6, \pi/3, \pi/2, 2\pi/3, 5\pi/6\}$ as $\{000, 001, 011, 111, 110, 100\}$. Then *SUM_XOR* and *OR_XOR* distances between $P(x, y), Q(x, y)$ are defined as following.

$$D_{SUM_XOR} = \frac{\sum_{y=1}^M \sum_{x=1}^N \sum_{i=1}^3 P_i^b(x, y) \otimes Q_i^b(x, y)}{3 * M * N} \quad (2)$$

$$D_{OR_XOR} = 1/(M * N) * \sum_{y=1}^M \sum_{x=1}^N ((P_0^b(x, y) \oplus Q_0^b(x, y)) | (P_1^b(x, y) \oplus Q_1^b(x, y)) | (P_2^b(x, y) \oplus Q_2^b(x, y))) \quad (3)$$

where M and N are the height and length of the pattern, $P_i^b(x, y), Q_i^b(x, y)$ are the i th bit plane of P and Q . \oplus denotes the bitwise exclusive OR (XOR), $|$ denotes the bitwise OR. Based on the five basic rules, denote by $a_i, i \in [0, 3]$ the number of pixels where the distance is $d_i, i \in [0, 3]$, (2),(3) can be rewritten as follows.

$$D_{SUM_XOR} = \frac{k_0 * a_0 + k_1 * a_1 + k_2 * a_2 + k_3 * a_3}{M * N} \quad (4)$$

$$= \frac{1/3 * a_1 + 2/3 * a_2 + 3/3 * a_3}{M * N} \quad (5)$$

$$D_{SUM_XOR} = \frac{k_0 * a_0 + k_1 * a_1 + k_2 * a_2 + k_3 * a_3}{M * N} \quad (6)$$

$$= \frac{1 * a_1 + 1 * a_2 + 1 * a_3}{M * N} \quad (7)$$

Here, $k_i, i \in 0, 1, 2, 3$ can be seen as the cost of wrong decision, and $k_0 = 0$. For a 6 orientation filter, k_i denotes the cost that the decision of θ_l while the ground truth is $\theta_{(l+i)mod6}$ or $\theta_{(l-i)mod6}$.

B. The Proposed Unified Distance Measure Scheme

In [20], Kong pointed out that *SUM_XOR* outperforms *OR_XOR* in PolyU palmprint databases. Compare (6) and (4), the difference between *OR_XOR* and *SUM_XOR* is that the using of different coefficients, which denotes the cost of wrong decision. Based on the comparison, we define the unified distance measure scheme between patterns $P(x, y)$ and $Q(x, y)$ as

$$D_u = \frac{k_1 * a_1 + k_2 * a_2 + k_3 * a_3}{M * N} \quad (8)$$

For a recognition task, the performance index are usually equal error rate (EER). For a two-choice decision task, equal error rate is the false reject rate equals the false accept rate. The EER is scale invariant with the distributions. Thus, the unified distance can be re-written as

$$D_u = \frac{k_1}{M * N} * (a_1 + \frac{k_2}{k_1} * a_2 + \frac{k_3}{k_1} * a_3) \quad (9)$$

$$D'_u = K_1 * a_1 + K_2 * a_2 + K_3 * a_3 \quad (10)$$

For the unified distance shown in (10), there are three parameters (K_1, K_2, K_3) to be determined, in which $K_1 = 1$. *SUM_XOR* and *OR_XOR* are two special cases, which take $K_2 = 2, K_3 = 3$ and $K_2 = 1, K_3 = 1$ respectively.

Optimization Problem The optimization problem can generally be stated as

$$\min eer = \min_{x=[K_2, K_3] \in \Omega} f(x), \quad (11)$$

where $f : \mathbb{R}^2 \rightarrow \mathbb{R}$ is a nonlinear function used for the computation of EER values, and Ω is the feasible region. For this optimization problem, to automatically determine the parameters of the unified distance measure model in (10), the heuristic algorithms, particle swarm optimization [22],

differential evolution [23] and firework algorithm [24] are used for the optimization, which are named as PSO-UDM, DE-UDM, FWA-UDM, respectively. Details about each heuristic algorithm can be found in the references provided below.

Particle Swarm Optimization (PSO, [25] [22]) mimics the process of the search for food of flocks. The particles (flocks) in the swarm move under the guidance of the cognitive information and social information

Differential Evolution(DE, [23]) maintains a population of candidate solutions while it also creates some new candidate solutions by combining existing ones according to its formulae. Then it keeps the candidate solution which has the best score or fitness on the optimization problem.

Fireworks Algorithm(FWA, [24])Inspired by the explosion of fireworks in the night sky, a firework explodes and generates the sparks in the nearby space can be seen as the search of an optimization problem.

III. EXPERIMENTS

To validate the performances of the proposed PSO-UDM, DE-UDM and FWA-UDM, three databases, the artificial data set, the PolyU palmprint database and the collected finger-vein database are used. POC, RLOC and CompCode are used for pattern extraction. The EER is compared to evaluate the performance. In the experiments, the search range of K_2 and K_3 are both set to $[0, 6]$.

To reduce the influences of shift and rotation of the patterns, in the matching part, a shift of $[-2, 2]$ in X axis and $[-2, 2]$ in Y axis is taken, and the minimal distance under a certain K_2, K_3 is recorded as the distance between two patterns.

Parameter Setup The swarm size for each algorithm is set to 50, and the maximum evaluation times is 5000.

- 1) PSO, $velocity_{max} = 20$, $c_1 = c_2 = 2$, $\omega = 0.5$, $\alpha = 1$
- 2) DE, the rest of parameters are same as [23]
- 3) FWA, the rest of parameters are same as [24]

The experimental platform for all experiments is Microsoft® Visual Studio 2010, based on an Intel(R) Core(TM) i7-2600 CPU @3.4GHz 3.7GHZ, 8GB RAM machine, running under Windows®7.

A. Experiments Using The Artificial Data Set

1) Experimental Design: The artificial database is composed by arbitrary images with 26 English letters (from "A" to "Z") and 10 Arabic numerals (from "0" to "9"). As pointed out in Section I, the orientation coding-based methods can effectively extract the line shape patterns, thus we design the data set, and use Gaussian noise and rotation to destroy the images. The σ and μ of the Gaussian kernel are set to 0 and 0.5, and the rotation angle is with probability from -5° to 5° . Ten samples of each original are randomly generated. The size of the images is 30×30 .

The experiment strategy is that: we first extract the patterns of the arbitrary images by orientation based pattern extraction algorithms, POC, RLOC and CompCode. Then, we get 360 patterns, with 36 classes. The three distances are computed among the date set, and *EER* is calculated. The total match

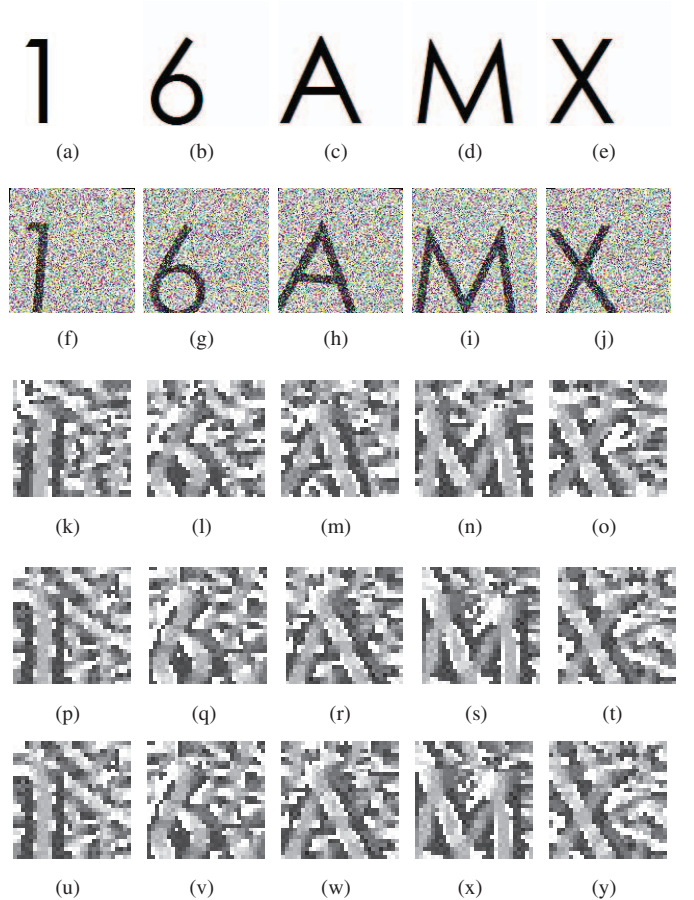


Fig. 1. Experiments on arbitrary images of English letters and Arabic numerals. (a)-(e) are the original images of the English Letters and Arabic numerals; (f)-(j) are the destroyed images of the English Letters and Arabic numerals; (k)-(o)are patterns extracted by POC; (p)-(t) are patterns extracted by RLOC; (u)-(y) are patterns generated by CompCode.

times is 64620, with 1620 genuine match times and 63000 imposter.

2) Experimental Results: Table I shows the experimental results, it can be seen that the proposed distance measure methods outperform both the *SUM_XOR* and *OR_XOR* on terms of equal error rate. Among the population based optimization methods on this data set, PSO-UDM gains the best performance for POC, RLOC and CompCode algorithms. PSO-UDM can reduce the EER by up to 18.6909% (5.69436E-02 to 4.63003E-02) for POC, 11.92% (7.63886E-02 to 6.72852E-02) for RLOC and 8.89% (8.33310E-02 to 7.59266E-02) for CompCode, respectively.

B. Experiments Using The PolyU Palmprint Database

1) Experimental Design: The PolyU palmprint database [26] is designed by The Hong Kong Polytechnic University, which contains palmprint images from 500 individuals. Each individual provides 12 images, each 6 images one time. Therefore, the database contains 6000 images from 500 individuals. The size of all the images is 128×128 .

First, the images are preprocessed for noises reduction and patterns are extracted by POC, RLOC and CompCode

TABLE I
EXPERIMENTAL RESULTS OF EER AND PARAMETERS OF K_2 , K_3 ON THE ARTIFICIAL DATA SET.

Distance	EER	POC		RLOC		CompCode		
		K_2	K_3	EER	K_2	K_3	EER	K_2
<i>OR_XOR</i>	5.69436E-02	1	1	7.63886E-02	1	1	8.33310E-02	1
<i>SUM_XOR</i>	7.77759E-02	2	3	8.74991E-02	2	3	8.47190E-02	2
PSO-UDM	4.63003E-02	0.728346	0.703715	6.72852E-02	1.219932	1.096775	7.59266E-02	1.138559
DE-UDM	5.06236E-02	0.543474	1.070833	7.59289E-02	0.728416	1.066439	7.71627E-02	1.41673
FWA-UDM	4.69185E-02	0.756903	0.76194	6.79032E-02	1.282784	1.02231	7.59275E-02	0.913847
								1.106167

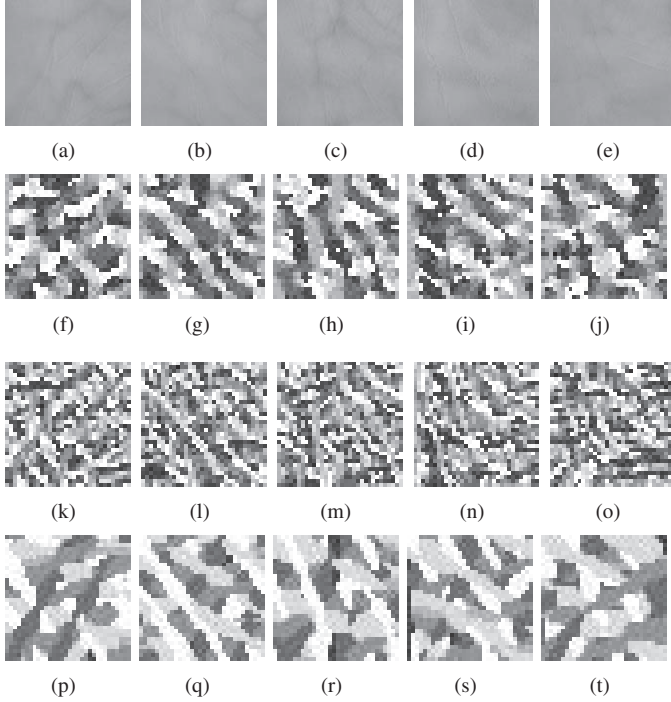


Fig. 2. Experiments on PolyU palmprint images database, (a)-(e) are the original palmprint images; (f)-(j) are patterns extracted by POC; (k)-(o) are patterns extracted by RLOC; (p)-(t) are patterns extracted by CompCode.

algorithms. Then the three distances are computed. There are totally 17997000 match times with 33000 genuine match time and 17964000 imposters. To reduce the computation load, the images are down sampled. Figure 2 illustrates the patterns extracted by POC, RLOC, and CompCode.

2) *Experimental Results:* Table II lists the results of EER, parameters of K_2 , K_3 introduced in the unified distance model. From the results, it can be concluded that the using of population based algorithms for parameters optimization for the unified distance model can achieve lower EER than *OR_XOR* and *SUM_XOR* on the palmprint database. Among the three methods, PSO-UDM, DE-UDM and FWA-UDM, PSO-UDM has the lowest EER which can reduce the EER by up to 7.88% (1.94250E-03 to 1.78942E-03) for POC, 7.52% (4.26636E-04 to 3.96492E-04) for RLOC, and 10.30% (2.36520E-03 to 2.12160E-03) for CompCode, respectively.

C. Experimental Using The Collected Finger-vein Database

1) *Experimental Design:* As pointed out previously, the orientation can effectively represent the line shape pattern, and finger-vein structure is one of them. Thus, we for the first time, use the orientation pattern for recognition. The finger-vein database contains 1500 images from 300 individuals, with 5 images each person, collected by an infrared CCD device. The size of all the images is 225×110 . As the collected images are destroyed by the noises, first the preprocessing work should be done. Gaussian filters are used to reduce the noise disturbance. To reduce the computation load, down sampling work is done, and all images are compressed to 112×55 . POC, RLOC, and CompCode algorithms are used to extract the patterns. For each algorithm, *SUM_XOR*, *OR_XOR* and the proposed distance measure methods are calculated. There are totally 1124250 match times, in which 3000 genuine match times and 112150 imposters.

2) *Experimental Results:* Experimental results are shown in Table III. First, we can see the POC, RLOC and CompCode can successfully extract the finger-vein patterns and achieve a high accuracy. Second, the proposed PSO-UDM, DE-UDM and FWA-UDM outperform the other two distance measure methods with lower equal error rate. Among these methods, PSO-UDM achieves the lowest EER value, which can reduce the EER by up to 1.63% (4.10087E-02 to 4.03393E-02) for POC, 7.79% (4.69999E-02 to 4.33401E-02) for RLOC and 2.59% (5.16752E-02 to 5.03389E-02) for CompCode, respectively.

IV. DISCUSSION

A. Performance Comparison

In this paper, the distance measure schemes for orientation patterns are detailed studied. We investigate the relation between hamming distance and angular distance, and based on the study, a unified distance is proposed. To validate the proposed distance methods, we test the orientation algorithms on three databases for recognition. Experimental results of EER shown in Table I, II, III, suggest that the proposed PSO-UDM, DE-UDM and FWA-UDM gain great advantages compared with the *OX_XOR* and *SUM_XOR* distance measure schemes. Among the three population based heuristic algorithms, PSO-UDM gains the best performance compared other two algorithms.

TABLE II
EXPERIMENTAL RESULTS OF EER AND PARAMETERS OF K_2 , K_3 ON THE POLYU PALMPrint DATABASE.

Distance	EER	POC		EER	RLOC		CompCode		
		K_2	K_3		K_2	K_3	EER	K_2	K_3
<i>OR_XOR</i>	2.21430E-03	1	1	4.26636E-04	1	1	2.36520E-03	1	1
<i>SUM_XOR</i>	1.94250E-03	2	3	4.28733E-04	2	3	2.88090E-03	2	3
PSO-UDM	1.78942E-03	2.796281	2.125603	3.96492E-04	1.766016	2.060412	2.12160E-03	0.714032	1.015583
DE-UDM	1.79121E-03	1.904904	2.03766	4.29041E-04	3.102268	3.356243	2.33845E-03	0.835902	1.483566
FWA-UDM	1.79072E-03	2.305181	1.878757	3.97389E-04	1.570431	1.461509	2.15388E-03	0.705089	0.854578

TABLE III
EXPERIMENTAL RESULTS OF EER AND PARAMETERS OF K_2 , K_3 ON THE COLLECTED FINGER-VEIN IMAGES.

Distance	EER	POC		EER	RLOC		CompCode		
		K_2	K_3		K_2	K_3	EER	K_2	K_3
<i>OR_XOR</i>	4.43410E-02	1	1	4.80010E-02	1	1	5.36720E-02	1	1
<i>SUM_XOR</i>	4.10087E-02	2	3	4.69999E-02	2	3	5.16752E-02	2	3
PSO-UDM	4.03393E-02	2.105049	2.171447	4.33401E-02	6	3.119498	5.03389E-02	2.654673	6
DE-UDM	4.03416E-02	2.200079	2.228645	4.33410E-02	6	3.1171	5.06735E-02	2.759301	6
FWA-UDM	4.03413E-02	2.019315	2.058841	4.33419E-02	5.829726	3.316062	5.06737E-02	2.918347	3.446459

B. Is *SUM_XOR* Always Better Than *OR_XOR* ?

From the results in Table I,II,III, we can see that *SUM_XOR* performs better in the collected finger-vein images database while *OR_XOR* gains better results in the artificial data set. We have discussed in Section II-A, that the K_i , $i \in [1, 3]$ are the costs of wrong decision. For a 6 orientation filter, K_i denotes the cost that the decision of θ_l while the ground truth is $\theta_{(l+i)mod6}$ or $\theta_{(l-i)mod6}$. Generally, it is believed that $K_1 \leq K_2 \leq K_3$, that higher difference between the decision value and the true value has higher costs. It is maybe the reason that *SUM_XOR* ($K_2 = 2$, $K_3 = 3$) is better than *OR_XOR* ($K_2 = 1$, $K_3 = 1$) in some cases. But in our experiments, it is not always so.

To investigate the relationship among K_1 , K_2 and K_3 , we conduct the experiments with the search range of K_2 and K_3 are both set to $[0, 6]$ with an interval of 0.1, $K_1 = 1$, and experiments under certain parameters are computed independently. Table IV lists some of the appropriate parameters for POC, RLOC and CompCode. Moreover, the parameters of K_2 and K_3 returned by PSO, DE and FWA can be found in Table I, II, III, it can be seen that it is not always $K_1 \leq K_2 \leq K_3$. Then, why? We think that the rotation, shift, non-linear transformation, and the distribution of the line shape structures that lead to these results. To investigate the influences of these operators and validate our ideas, two tests are designed and conducted.

The first test is to study the changes of the responses of the convolution of images with filters $G(x, y, \theta)$. θ is from 1° to 180° at 1° intervals. In Figure 4(a)-(f), two lines (sample1, sample2) mean they are the convolution results $I(x, y) \otimes G(x, y, \theta)$ from two samples of one individual. We can see that even though they are from the same individual, maybe the responses are quite different due to the noise, shift, rotation, etc. In addition, the response line with the θ may be a float curve, or not a uni-modal function. All these factors may lead to the suffering of the risk of wrong decision.

TABLE IV
LISTS OF SOME OF APPROPRIATE PARAMETERS FOR POC, RLOC AND COMPCode ALGORITHMS ($K_1 = 1$)

	Database	Parameters
POC	PolyU palmprint database	$K_2 = 2.8$, $K_3 = 1.1$
	finger-vein images	$K_2 = 2.1$, $K_3 = 2.1$
	artificial data set	$K_2 = 0.6$, $K_3 = 0.8$
RLOC	PolyU palmprint database	$K_2 = 1.6$, $K_3 = 1.8$
	finger-vein images	$K_2 = 5.8$, $K_3 = 3.4$
	artificial data set	$K_2 = 1.5$, $K_3 = 1.3$
CompCode	PolyU palmprint database	$K_2 = 0.7$, $K_3 = 1.0$
	finger-vein images	$K_3 = 1.4$, $K_2 = 3.5$
	artificial data set	$K_2 = 1.0$, $K_3 = 1.1$

Second, we investigate a special case, that the convolution with a artificial arbitrary image. In the palmprint image and finger-vein image, there are a lot of intersection regions of two lines as shown in Fig 4(g)-(h). For POC, RLOC and CompCode, they cannot deal with these situations effectively. The responses of convolution of the intersect point with θ is a multi-modal curve, which makes the final encoded orientation is easily influenced by the noises. Thus, we conclude that, $K_1 \leq K_2 \leq K_3$ is now always necessary, on account of the noise, rotation, shift and the intersection regions.

V. CONCLUSION

In this paper, we studied the distance measure schemes for orientation coding-based patterns and presented the relation between hamming distance and angular distance. Based on the analysis of the relationship, a unified distance measure scheme is proposed, in which hamming distance and angular distance are two special cases. To determine the parameters introduced in the unified distance model, population based heuristic algorithms, PSO, DE, and FWA were used for the optimization. Experimental results on three data bases suggested that the proposed PSO-UDM, DE-UDM and FWA-UDM can achieve lower EER. Moreover, we investigated the

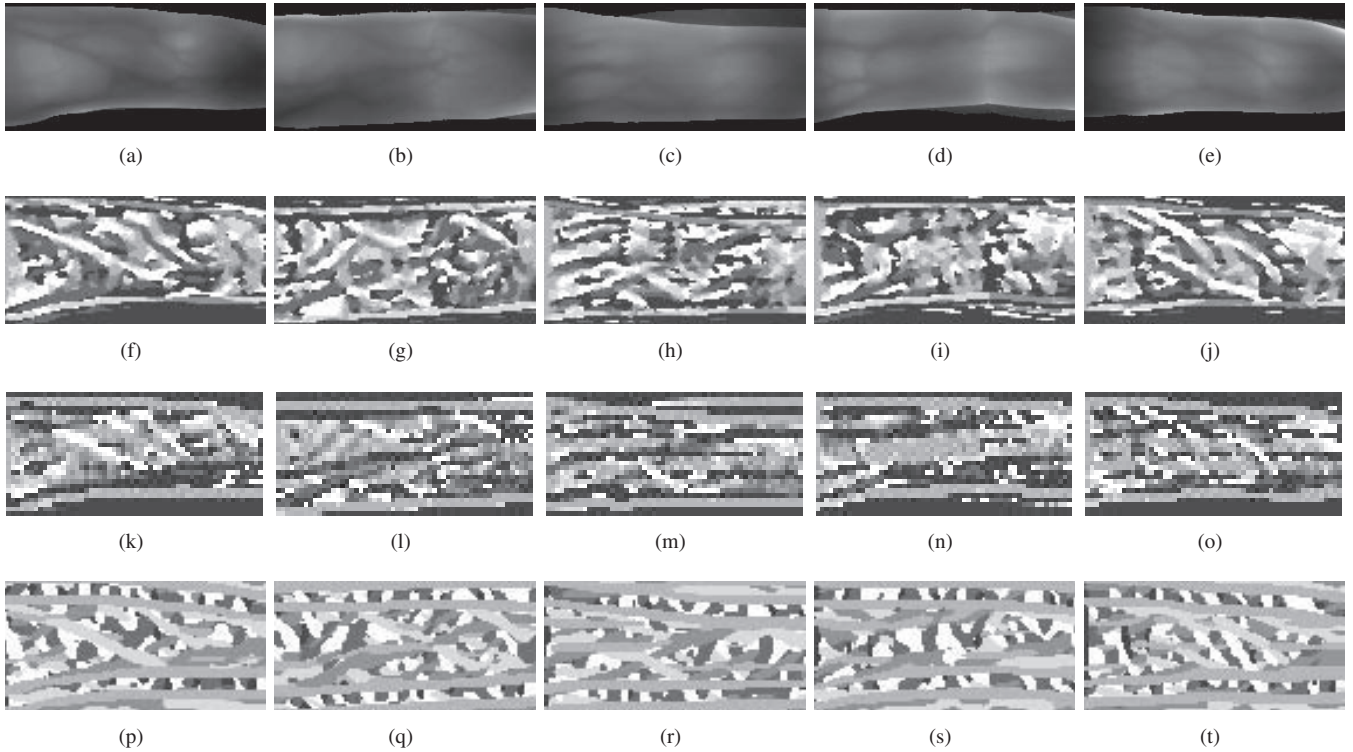


Fig. 3. Experiments on the collected finger-vein images. (a)-(e) are the original images of the finger-vein images; (f)-(j) are patterns extracted by POC; (k)-(o) are patterns extracted by RLOC; (p)-(t) are patterns extracted by CompCode.

influences of parameters in the unified distance model, and present an explanation why $K_1 \leq K_2 \leq K_3$ is not always necessary.

REFERENCES

- [1] P. Phillips, H. Moon, S. Rizvi, and P. Rauss, "The feret evaluation methodology for face-recognition algorithms," *Pattern Analysis and Machine Intelligence, IEEE Transactions on*, vol. 22, no. 10, pp. 1090–1104, 2000.
- [2] J. Daugman, "The importance of being random: statistical principles of iris recognition," *Pattern recognition*, vol. 36, no. 2, pp. 279–291, 2003.
- [3] D. Zhang, W. Kong, J. You, and M. Wong, "Online palmprint identification," *Pattern Analysis and Machine Intelligence, IEEE Transactions on*, vol. 25, no. 9, pp. 1041–1050, 2003.
- [4] G. Lu, D. Zhang, and K. Wang, "Palmprint recognition using eigenpalms features," *Pattern Recognition Letters*, vol. 24, no. 9, pp. 1463–1467, 2003.
- [5] A. Jain, L. Hong, and R. Bolle, "On-line fingerprint verification," *Pattern Analysis and Machine Intelligence, IEEE Transactions on*, vol. 19, no. 4, pp. 302–314, 1997.
- [6] L. Rabiner, "A tutorial on hidden markov models and selected applications in speech recognition," *Proceedings of the IEEE*, vol. 77, no. 2, pp. 257–286, 1989.
- [7] N. Miura, A. Nagasaka, and T. Miyatake, "Feature extraction of finger-vein patterns based on repeated line tracking and its application to personal identification," *Machine Vision and Applications*, vol. 15, no. 4, pp. 194–203, 2004.
- [8] —, "Extraction of finger-vein patterns using maximum curvature points in image profiles," *IEICE transactions on information and systems*, vol. 90, no. 8, pp. 1185–1194, 2007.
- [9] T. Yanagawa, S. Aoki, and T. Ohyama, "Human finger vein images are diverse and its patterns are useful for personal identification," 2007-12, 2007.
- [10] W. Yang, X. Yu, and Q. Liao, "Personal authentication using finger vein pattern and finger-dorsum texture fusion," in *Proceedings of the 17th ACM international conference on Multimedia*. ACM, 2009, pp. 905–908.
- [11] B. Huang, Y. Dai, R. Li, D. Tang, and W. Li, "Finger-vein authentication based on wide line detector and pattern normalization," in *Pattern Recognition (ICPR), 2010 20th International Conference on*. IEEE, 2010, pp. 1269–1272.
- [12] J. Yang and X. Li, "Efficient finger vein localization and recognition," in *Pattern Recognition (ICPR), 2010 20th International Conference on*. IEEE, 2010, pp. 1148–1151.
- [13] A. Kumar and Y. Zhou, "Human identification using finger images," *Image Processing, IEEE Transactions on*, vol. 21, no. 4, pp. 2228–2244, 2012.
- [14] W. Song, T. Kim, H. Kim, J. Choi, H. Kong, and S. Lee, "A finger-vein verification system using mean curvature," *Pattern Recognition Letters*, vol. 32, no. 11, pp. 1541–1547, 2011.
- [15] Z. Zhang, S. Ma, and X. Han, "Multiscale feature extraction of finger-vein patterns based on curvelets and local interconnection structure neural network," in *Pattern Recognition, 2006. ICPR 2006. 18th International Conference on*, vol. 4. IEEE, 2006, pp. 145–148.
- [16] J. Wu and C. Liu, "Finger vein pattern identification using principal component analysis and the neural network technique," *Expert Systems with Applications*, vol. 38, no. 5, pp. 5423–5427, 2011.
- [17] A. Kong and D. Zhang, "Competitive coding scheme for palmprint verification," in *Pattern Recognition, 2004. ICPR 2004. Proceedings of the 17th International Conference on*, vol. 1. IEEE, 2004, pp. 520–523.
- [18] W. Jia, D. Huang, and D. Zhang, "Palmprint verification based on robust line orientation code," *Pattern Recognition*, vol. 41, no. 5, pp. 1504–1513, 2008.
- [19] X. Wu, K. Wang, and D. Zhang, "Palmprint authentication based on orientation code matching," in *Audio-and Video-Based Biometric Person Authentication*. Springer, 2005, pp. 83–132.
- [20] A. Kong, "Palmprint identification based on generalization of iriscode," Ph.D. dissertation, University of Waterloo, 2007.
- [21] Z. Guo, W. Zuo, L. Zhang, and D. Zhang, "A unified distance measurement for orientation coding in palmprint verification," *Neurocomputing*, vol. 73, no. 4, pp. 944–950, 2010.
- [22] D. Bratton and J. Kennedy, "Defining a standard for particle swarm optimization," in *Swarm Intelligence Symposium, 2007. SIS 2007. IEEE*. IEEE, 2007, pp. 120–127.

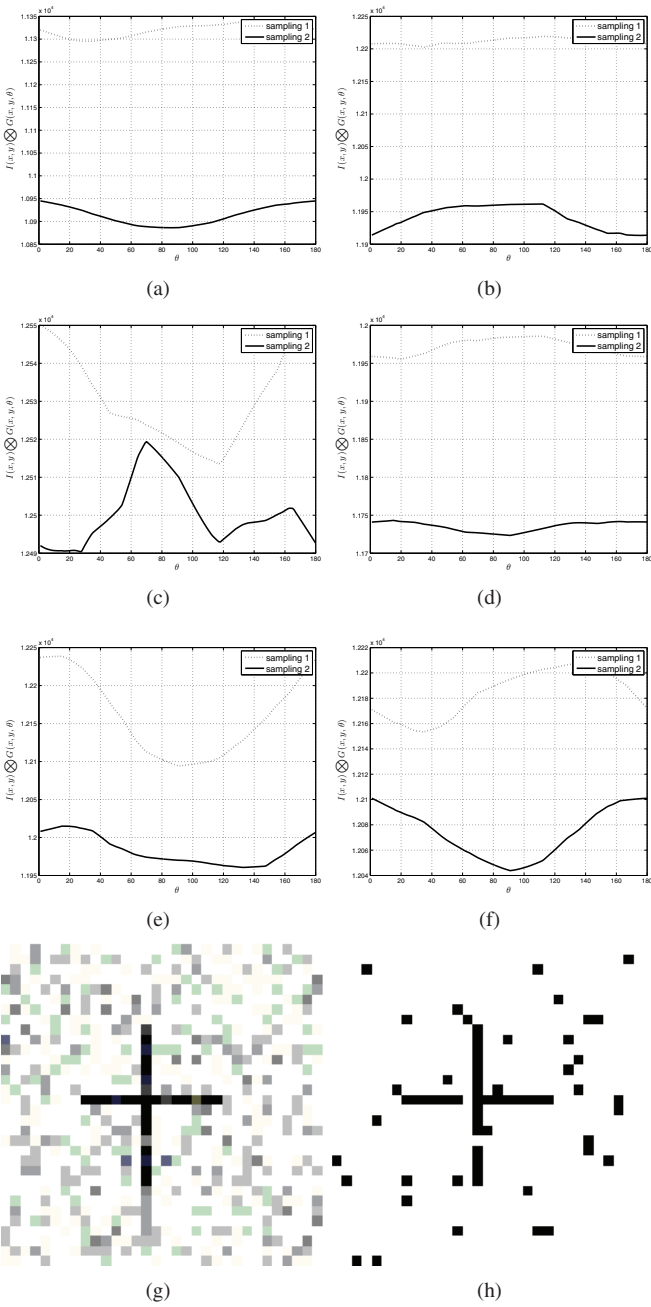


Fig. 4. (a)-(f) Response comparison between two sampling palmprint images of one individual from 0° to 180° ; (g)-(h) Synthesized images with Gaussian noise and salt & pepper noise.

- [23] R. Storn and K. Price, "Differential evolution—a simple and efficient heuristic for global optimization over continuous spaces," *Journal of global optimization*, vol. 11, no. 4, pp. 341–359, 1997.
- [24] Y. Tan and Y. Zhu, "Fireworks algorithm for optimization," *Advances in Swarm Intelligence*, pp. 355–364, 2010.
- [25] J. Kennedy and R. Eberhart, "Particle swarm optimization," in *Neural Networks, 1995. Proceedings., IEEE International Conference on*, vol. 4. IEEE, 1995, pp. 1942–1948.
- [26] "Polyu palmprint database." [Online]. Available: <http://www.comp.polyu.edu.hk/biometrics/MultispectralPalmpprint/MSP.htm>